Contribution from the Dipartimento di Chimica, Università di Siena, Pian dei Mantellini, 44, 53100 Siena, Italy, and Department of Chemistry, University of Virginia, McCormick Road, Charlottesville, Virginia 22901

Metal Complexes of the Antiinflammatory Drug Piroxicam

Renzo Cini,*[†] Gianluca Giorgi,[†] Arnaldo Cinquantini,[†] Claudio Rossi,[†] and Michal Sabat*[‡]

Received December 8, 1988

The synthesis and characterization of Fe(II), Co(II), Ni(II), Cu(II), Zn(II), and Cd(II) complexes with a potent antiinflammatory drug piroxicam [4-hydroxy-2-methyl-*N*-2-pyridyl-2*H*-1,2-benzothiazine-3-carboxamide 1,1-dioxide] are described. The crystal and molecular structures of $M(Pir)_2(DMF)_2$ (M = Cu, Cd; Pir = piroxicam; DMF = *N*,*N*-dimethylformamide) are also reported. Crystallographic data are as follows: $Cd(Pir)_2(DMF)_2$, monoclinic, $P2_1/c$, a = 9.890 (2) Å, b = 8.076 (2) Å, c = 24.998 (4) Å, β = 100.16 (2)°, Z = 2. The structure was refined to $R(F_o)$ = 0.039 for 2321 reflections with $I > 3\sigma(I)$. $Cu(Pir)_2(DMF)_2$, monoclinic, $P2_1/c$, a = 10.142 (2) Å, b = 7.855 (3) Å, c = 24.053 (4) Å, β = 97.79 (2)°, Z = 2. The refinement yielded the final $R(F_o)$ of 0.059 for 797 reflections with $I > 3\sigma(I)$. Both Cd(II) and Cu(II) ions bind to the piroxicam molecule through its amide O and pyridyl N atoms.

Introduction

A variety of recent observations indicated that copper complexes when administered in conjunction with antiinflammatory drugs exhibit synergistic activity.[1] It has also been found that the Cu complexes of some antiarthritic drugs are themselves more active as antiinflammatory agents than their parent compounds.[2,3] The molecular basis of action of the Cu complexes with well-established drugs such as $Cu(salicylate)_2$ is not as yet clear.

We therefore have undertaken the investigation of the interaction of Cu(II) and other first-row transition-metal ions with a widely used antiinflammatory drug from the carboxamide family, namely piroxicam[4] (I). Potentially, piroxicam may act as a

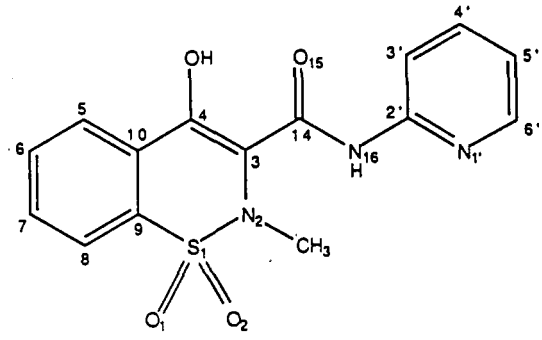

I

multiple-site ligand and various schemes of its bonding to metal ions could be considered. Recent reports[5,6] on metal complexes with other therapeutic agents of the same class suggested that the drugs act as chelate ligands with coordination involving the enolate oxygen atom and the oxygen atom of the amido group. In contrast, we show here that piroxicam prefers a coordination mode employing the pyridyl group of the side chain and the amide oxygen atom.

Experimental Section

Chemicals. Crude piroxicam (Pfizer Italiana S.p.A.) was recrystallized twice from CH_3OH. Analytical grade cobalt(II) acetate tetrahydrate, copper(II) acetate monohydrate, zinc(II) acetate dihydrate, and cadmium(II) acetate dihydrate (Merck) were used without any purification. Reagent grade nickel(II) acetate tetrahydrate (Merck) was recrystallized twice from water. Iron(II) acetate tetrahydrate was prepared as follows. A mixture containing 6.60 g of analytical grade glacial acetic acid (Merck; 0.11 mol) and 50 mL of water was deaerated by bubbling for 0.5 h with ultrapure argon passed through an OXY-TRAP column (Alltech Associates) with 1/4-in. fittings; 2.79 g (0.05 mol) of ultrapure iron wire (Aldrich; 0.25-mm diameter, 99.998%) was added to the acetic acid solution, and the mixture was stirred at 60–70 °C to complete dissolution of the metal. The green solution was dried, and the excess of acetic acid was removed under vacuum by a stream of deoxygenated argon at about 60 °C. The pale green powder was stored under argon in sealed glass vials. Analytical data of the iron content are in agreement with four molecules of water of crystallization. The salt was used without any further purification.

Synthesis of the Complexes. The Co(II), Ni(II), Cu(II), Zn(II), and Cd(II) piroxicam derivatives were prepared according to the following procedure. Hot methanol solutions of the ligand (30 mL, 1.0 mmol) were mixed with hot methanol solutions of the metal acetate (5 mL, 0.5 mmol). The mixtures were refluxed under stirring for about 0.5 h. The complexes precipitate as microcrystalline powders after a few minutes of mixing. The solid compounds were filtered, washed with hot methanol, and then dried under vacuum at room temperature for 24 h. The powders were recrystallized from DMSO (dimethyl sulfoxide) as well as from DMF (*N*,*N*-dimethylformamide). The Co(II), Ni(II), Cu(II), Zn(II), and Cd(II) derivatives gave pink, pale green, dark green, yellow, and yellow crystals, respectively.

The yields were about 60–70%. The analytical data for C, H, N, S, and M (M = metal) show that the crystals can be formulated as $M(Pir)_2 \cdot mA \cdot nH_2O$, A = DMSO or DMF. m and n range between 0 and 2 and 0 and 4, respectively; they depend on the metal ions as well as on the crystallization and storage conditions.

The Co(II), Ni(II), and Cu(II) derivatives show clear thermochromic effects. As an example, the green $Ni(Pir)_2 \cdot 2DMSO \cdot 2H_2O$ crystalline powder turns reversibly to red at about 170 °C. At 280 °C the red solid decomposes. A similar behavior was also revealed for the Co(II) and Cu(II) derivatives. The Co(II) species can be handled without any particular care in the solid state and in DMSO or DMF solution.

The Fe(II) derivative was obtained by using the following method. A mixture containing the ligand (1.0 mmol) and methanol (30 mL) was deaerated by bubbling argon previously passed through an OXY-TRAP column for 0.5 h.

The mixture was heated up to complete dissolution of the ligand. A 0.5-mmol sample of the solid iron(II) acetate tetrahydrate was added to the hot solution under a stream of argon. A microcrystalline orange powder precipitated after a few minutes. The mixture was refluxed under argon for about 0.5 h. The crystalline solid was filtered and washed with deaerated hot methanol under argon; then it was dried in the vacuum at room temperature for 48 h. The resulting solid was stable in air for many days. It is fairly soluble in DMSO, DMF, and THF (tetrahydrofuran), but the solutions turn red very quickly in air. The analytical data are in agreement with the formula $Fe(Pir)_2 \cdot 4H_2O$. Anal. Calcd for $C_{30}H_{32}N_6O_{12}FeS_2$: C, 45.69; H, 4.09; N, 10.66; Fe, 7.08; S, 8.13. Found: C, 46.08; H, 4.07; N, 10.20; Fe, 7.3; S, 7.77.

The orange crystalline powder turns irreversibly dark brown at about 100 °C due to a change in the oxidation state of the metal ion.

Spectroscopic and Magnetic Measurements. NMR data were recorded on a Varian XL-200 spectrometer operating at 50.03 MHz for the ^{13}C

[†] Università di Siena.
[‡] University of Virginia.

(1) Crouch, R. K.; Kensler, T. W.; Oberley, L. W.; Sorenson, J. R. J. In *Biological and Inorganic Copper Chemistry*; Karlin, K. D., Zubieta, J., Eds.; Adenine Press: Guilderland, NY, 1985; Vol. 1, pp 139–157.
(2) (a) Sorenson, J. R. J. *J. Med. Chem.* **1976**, *19*, 135. (b) Sorenson, J. R. J. In *Inflammatory Diseases and Copper*; Sorenson, J. R. J., Ed.; Humana Press: Clifton, NJ, 1982; pp 289–299.
(3) Brown, D. H.; Smith, W. E.; Teape, J. W.; Lewis, A. J. *J. Med. Chem.* **1980**, *23*, 729.
(4) Piroxicam = 4-hydroxy-2-methyl-*N*-2-pyridyl-2*H*-1,2-benzothiazine-3-carboxamide 1,1-dioxide (hereafter HPir). The antiinflammatory properties of the drug known also as felden (Pfizer) have been described: Lombardino, J. G.; Wiseman, E. H.; Chiaini, J. *J. Med. Chem.* **1973**, *16*, 493.
(5) Harrison, D. O.; Thomas, R.; Underhill, A. E.; Fletcher, J. K.; Gomm, P. S.; Hallway, F. *Polyhedron* **1985**, *4*, 681.
(6) Bury, A.; Underhill, A. E.; Kemp, D. R.; O'Shea, N. J.; Smith, J. P.; Gomm, P. S.; Gomm, P. S. *Inorg. Chim. Acta* **1987**, *138*, 85.

0020-1669/90/1329-5197$02.50/0

Table I. Crystallographic Data for $M(Pir)_2(DMF)_2$

Cd Complex	
$C_{36}H_{38}N_8O_{10}S_2Cd$	$T = -120$ °C
fw = 919.23	$\lambda = 0.71069$ Å
$a = 9.890$ (2) Å	$d_{calcd} = 1.55$ g cm^{-3}
$b = 8.076$ (2) Å	$\mu = 7.18$ cm^{-1}
$c = 24.998$ (4) Å	transm coeff = 0.89–1.12
$\beta = 100.16$ (2)°	3724 unique reflections
$V = 1965$ (1) Å^3	2321 reflections with $I > 3\sigma(I)$
$Z = 2$	$R(F_o) = 0.039$
$P2_1/c$, No. 14	$R_w(F_o) = 0.048$
Cu Complex	
$C_{36}H_{38}N_8O_{10}S_2Cu$	$T = -120$ °C
fw = 870.41	$\lambda = 0.71069$ Å
$a = 10.142$ (2) Å	$d_{calcd} = 1.52$ g cm^{-3}
$b = 7.855$ (3) Å	$\mu = 7.47$ cm^{-1}
$c = 24.053$ (4) Å	transm coeff = 0.77–1.13
$\beta = 97.79$ (2)°	2701 unique reflections
$V = 1899$ (2) Å^3	797 reflections with $I > 3\sigma(I)$
$Z = 2$	$R(F_o) = 0.059$
$P2_1/c$, No. 14	$R_w(F_o) = 0.063$

nucleus. Spin–lattice relaxation rate measurements were obtained by using the $(180°-\tau-90°-t)_n$ pulse sequence. The experimental error for the reported R_{1p} values was found to be within 5%. The experiments were performed at 70 °C to avoid slow-exchange equilibria, which affect the NMR line widths and preclude the accurate determination of the spin–lattice relaxation rates of some carbon nuclei such as C(3), C(4), C(10), and C(6′). The paramagnetic contribution, R_{1p}, was obtained from the equation: $R_{1p} = R_{1exp} - R_{1blank}$, where R_{1exp} and R_{1blank} are the relaxation rates measured in paramagnetic and diamagnetic systems, respectively.

Infrared spectra for the complexes in the solid state, as Nujol mulls between CsI plates or as KBr pellets, were measured on a Perkin-Elmer Model 597 spectrometer. Ultraviolet and visible spectra were recorded on a Perkin-Elmer model 200 spectrophotometer equipped with a Hitachi recorder; 1-cm path length quartz cells were used for all the determinations in solution. Reflectance spectra for the solid compounds were obtained from a thin layer of powder smeared on a S&S filter paper strip.

Magnetic susceptibility values were measured by the Faraday method at 24 °C, using $CuSO_4 \cdot 5H_2O$ as reference. For the diamagnetic correction of molar susceptibility, the value $\chi_{dia} = 433.12 \times 10^{-6}$ cgsu was used. The effective magnetic moment (μ_{eff}) values were calculated by using the Curie equation: $\mu_{eff} = 2.83(\chi_M^{corr})^{1/2}T^{1/2}$.

X-ray Diffraction Studies of $M(Pir)_2(DMF)_2$ (M = Cu, Cd). X-ray-quality crystals of the Cu and Cd complexes were obtained from DMF solutions at room temperature. A summary of the crystallographic data is presented in Table I. All measurements were performed at −120 °C on an Enraf-Nonius CAD4 diffractometer using Mo Kα radiation (λ = 0.71069 Å). Accurate cell parameters were determined by least-squares refinement of 25 high-angle reflections. Intensities of four standard reflections were monitored every 3 h of X-ray exposure showing no significant decay. All calculations were performed by using the TEXSAN 5.0 crystallographic software package[7] on a MicroVAX 3600 computer and in a later stage on a VAXstation II/RC. Absorption corrections were introduced by applying the DIFABS program.[8]

$Cd(Pir)_2(DMF)_2$. A crystal of dimensions 0.37 × 0.28 × 0.22 mm was used for the data collection up to $2\theta = 50°$. The structure was solved by using heavy-atom methods (Patterson and Fourier techniques). The full-matrix least-squares refinement with anisotropic thermal parameters for the non-hydrogen atoms yielded the final R of 0.039 ($R_w = 0.048$) for 2321 reflections with $I > 3\sigma(I)$.

The H atoms were located on the difference Fourier maps and were included in the final refinement as fixed contributors to the structure factors. The largest peak in the final difference map was 0.48 e/Å^3 high. Final positional parameters are listed in Table II.

$Cu(Pir)_2(DMF)_2$. Crystals of the compound grew as very tiny needles. Many trials to grow larger crystals failed, and only a very small crystal of dimensions 0.18 × 0.02 × 0.02 mm could be selected for the X-ray measurements. The crystal diffracted very weakly, and no significant intensities were observed above $2\theta = 45°$. The positional parameters of the Cd complex were applied as the starting model in the full-matrix least-squares refinement with anisotropic thermal parameters for the Cu and S atoms. The final R factor was 0.059 ($R_w = 0.063$) for 797 reflections with $I > 3\sigma(I)$. The final difference map was featureless with the highest peak of 0.43 e/Å^3. Final positional parameters are listed in Table III.

(7) *TEXSAN: Single crystal Structure Analysis Software*; Version 5.0; Molecular Structure Corp.: The Woodlands, TX, 1989.
(8) Walker, N.; Stuart, D. *Acta Crystallogr.* **1983**, *A39*, 158.

Table II. Positional Parameters for $Cd(Pir)_2(DMF)_2$

atom	x	y	z
Cd	0	0	0
S(1)	−0.2584 (1)	0.1415 (2)	0.19686 (5)
O(1)	−0.3718 (4)	0.0881 (5)	0.1571 (1)
O(2)	−0.2126 (4)	0.0369 (4)	0.2428 (1)
O(5)	0.2282 (3)	0.1047 (5)	0.0075 (1)
O(15)	−0.0413 (3)	0.1334 (4)	0.0719 (1)
O(17)	−0.2646 (4)	0.5573 (4)	0.0956 (2)
N(1′)	−0.0767 (4)	0.2395 (5)	−0.0429 (2)
N(2)	−0.1301 (4)	0.1782 (5)	0.1662 (2)
N(7)	0.4277 (4)	0.1816 (6)	−0.0175 (2)
N(16)	−0.1525 (4)	0.3685 (5)	0.0325 (2)
C(2′)	−0.1329 (4)	0.3676 (6)	−0.0212 (2)
C(3)	−0.1615 (5)	0.3011 (6)	0.1237 (2)
C(3′)	−0.1789 (5)	0.5101 (7)	−0.0518 (2)
C(4)	−0.2331 (5)	0.4454 (7)	0.1316 (2)
C(4′)	−0.1661 (5)	0.5146 (8)	−0.1059 (2)
C(5)	−0.3070 (5)	0.6300 (7)	0.2011 (2)
C(5′)	−0.1068 (6)	0.3824 (7)	−0.1283 (2)
C(6)	−0.3482 (5)	0.6574 (8)	0.2511 (3)
C(6′)	−0.0632 (5)	0.2490 (7)	−0.0960 (2)
C(7)	−0.3602 (5)	0.5257 (7)	0.2848 (2)
C(8)	−0.3336 (5)	0.3647 (8)	0.2694 (2)
C(9)	−0.2930 (5)	0.3409 (7)	0.2194 (2)
C(10)	−0.2786 (5)	0.4714 (6)	0.1847 (2)
C(13)	0.0077 (5)	0.1860 (7)	0.1999 (2)
C(14)	−0.1138 (5)	0.2590 (6)	0.0748 (2)
C(15)	0.3010 (5)	0.1193 (6)	−0.0272 (2)
C(16)	0.5071 (5)	0.2001 (7)	−0.0610 (2)
C(17)	0.4883 (5)	0.2449 (7)	0.0355 (2)

Table III. Positional Parameters for $Cu(Pir)_2(DMF)_2$

atom	x	y	z
Cu	0	0	0
S(1)	−0.2471 (4)	0.0888 (6)	0.2023 (2)
O(1)	−0.3571 (1)	0.032 (1)	0.1632 (4)
O(2)	−0.2004 (9)	−0.019 (2)	0.2490 (4)
O(5)	0.229 (1)	0.099 (1)	0.0142 (4)
O(15)	−0.037 (1)	0.107 (1)	0.0680 (4)
O(17)	−0.2740 (9)	0.523 (2)	0.0987 (4)
N(1′)	−0.054 (1)	0.218 (2)	−0.0439 (5)
N(2)	−0.126 (1)	0.138 (1)	0.1672 (5)
N(7)	0.427 (1)	0.198 (2)	−0.0089 (5)
N(16)	−0.154 (1)	0.340 (2)	0.0299 (5)
C(2′)	−0.123 (1)	0.349 (2)	−0.0242 (6)
C(3)	−0.161 (1)	0.266 (2)	0.1235 (6)
C(3′)	−0.162 (1)	0.489 (3)	−0.0560 (5)
C(4)	−0.238 (1)	0.410 (2)	0.1347 (6)
C(4′)	−0.133 (1)	0.496 (3)	−0.1096 (6)
C(5)	−0.317 (2)	0.588 (2)	0.2103 (7)
C(5′)	−0.061 (2)	0.370 (2)	−0.1308 (6)
C(6)	−0.357 (2)	0.604 (2)	0.2628 (7)
C(6′)	−0.021 (1)	0.233 (2)	−0.0972 (6)
C(7)	−0.360 (1)	0.469 (2)	0.2972 (6)
C(8)	−0.324 (2)	0.307 (2)	0.2802 (7)
C(9)	−0.290 (2)	0.284 (2)	0.2284 (6)
C(10)	−0.283 (1)	0.428 (2)	0.1919 (6)
C(13)	0.010 (2)	0.148 (2)	0.1992 (6)
C(14)	−0.113 (1)	0.231 (2)	0.0730 (6)
C(15)	0.304 (2)	0.131 (2)	−0.0216 (7)
C916)	0.509 (2)	0.227 (3)	−0.0523 (8)
C(17)	0.484 (2)	0.230 (3)	0.0472 (8)

Results and Discussion

Structure of the Cu and Cd Complexes. Pertinent bond lengths and angles for the Cd and Cu derivatives are shown in Table IV. The molecular structure of the Cd complex is presented in Figure 1. The Cu complex is isostructural with and shows geometrical features similar to the Cd complex. The six-coordinate metal ion sits upon crystallographic centers of symmetry with the piroxicam ligand chelated through its carbonyl oxygen atom O(15) of the amido group and the pyridyl nitrogen atom N(1′). The axial positions are occupied by two DMF molecules bonded to the metal

Table IV. Selected Bond Lengths (Å) and Angles (deg) for $M(Pir)_2(DMF)_2$

	M = Cd	M = Cu
(a) Coordination Sphere		
M–O(5)	2.386 (3)	2.43 (1)
M–O(15)	2.194 (3)	1.92 (1)
M–N(1′)	2.276 (4)	2.05 (1)
O(5)–M–O(15)	94.1 (1)	91.8 (4)
O(5)–M–N(1′)	88.2 (1)	90.8 (4)
O(15)–M–N(1′)	82.7 (1)	90.2 (5)
(b) Piroxicam Ligand		
S(1)–O(1)	1.428 (3)	1.43 (1)
S(1)–O(2)	1.434 (4)	1.44 (1)
S(1)–N(2)	1.623 (4)	1.63 (1)
N(2)–C(13)	1.473 (6)	1.48 (2)
N(2)–C(3)	1.446 (6)	1.46 (2)
C(3)–C(4)	1.396 (7)	1.42 (2)
C(4)–O(17)	1.276 (6)	1.25 (2)
C(4)–C(10)	1.489 (7)	1.52 (2)
C(10)–C(9)	1.388 (7)	1.44 (2)
C(9)–S(1)	1.759 (6)	1.73 (2)
C(3)–C(14)	1.427 (7)	1.40 (2)
C(14)–N(16)	1.380 (6)	1.37 (2)
N(16)–C(2′)	1.390 (2)	1.38 (2)
C(2′)–C(3′)	1.413 (7)	1.36 (2)
C(3′)–C(4′)	1.379 (7)	1.36 (2)
C(4′)–C(5′)	1.383 (8)	1.37 (2)
C(5′)–C(6′)	1.371 (8)	1.37 (2)
C(6′)–N(1′)	1.359 (6)	1.37 (2)
N(1′)–C(2′)	1.333 (6)	1.37 (2)
O(1)–S(1)–O(2)	118.6 (2)	118.4 (7)
C(9)–S(1)–N(2)	101.3 (2)	103.0 (7)
S(1)–N(2)–C(3)	112.9 (3)	114 (1)
N(2)–C(3)–C(4)	121.1 (5)	120 (1)
C(3)–C(4)–C(10)	119.1 (5)	119 (1)
C(4)–C(10)–C(9)	122.0 (5)	122 (1)
C(10)–C(9)–S(1)	116.6 (4)	116 (1)
N(2)–C(3)–N(16)	113.8 (4)	114 (1)
N(16)–C(14)–O(15)	124.0 (5)	123 (1)
C(14)–N(16)–C(2′)	132.0 (5)	131 (1)
C(2′)–C(3′)–C(4′)	118.3 (5)	119 (2)
C(3′)–C(4′)–C(5′)	119.7 (5)	121 (2)
C(4′)–C(5′)–C(6′)	118.7 (5)	118 (2)
C(5′)–C(6′)–N(1′)	123.1 (5)	122 (2)
C(6′)–N(1′)–C(2′)	118.2 (4)	117 (1)
(c) DMF Ligand		
O(5)–C(15)	1.229 (6)	1.25 (2)
C(15)–N(7)	1.332 (6)	1.35 (2)
N(7)–C(16)	1.455 (7)	1.44 (2)
N(7)–C(17)	1.449 (7)	1.42 (2)
M–O(5)–C(15)	130.3 (3)	129 (1)
O(5)–C(15)–N(7)	123.9 (5)	123 (2)
C(16)–N(7)–C(17)	117.1 (4)	117 (1)

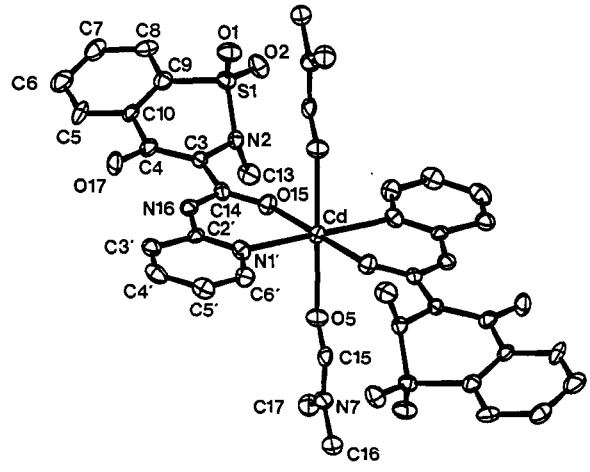

Figure 1. ORTEP drawing of the $Cd(Pir)_2(DMF)_2$ molecule showing the atom-labeling scheme and 50% probability thermal ellipsoids.

Table V. Structural Characteristics of Piroxicam in Various Forms[a]

	I	II	III	IV	V
Bond Lengths (Å)					
N(2)–C(3)	1.427 (4)	1.445 (6)	1.441 (4)	1.446 (6)	1.46 (2)
C(3)–C(4)	1.369 (4)	1.396 (6)	1.387 (5)	1.397 (7)	1.42 (2)
C(3)–C(14)	1.463 (4)	1.429 (6)	1.446 (5)	1.427 (7)	1.40 (2)
C(4)–C(10)	1.462 (4)	1.500 (6)	1.498 (5)	1.489 (7)	1.52 (2)
C(4)–O(17)	1.341 (4)	1.279 (5)	1.280 (4)	1.276 (6)	1.25 (2)
C(14)–O(15)	1.238 (4)	1.240 (5)	1.240 (4)	1.252 (6)	1.25 (2)
C(14)–N(16)	1.353 (4)	1.385 (6)	1.365 (4)	1.380 (6)	1.37 (2)
N(16)–C(2′)	1.408 (4)	1.368 (6)	1.394 (4)	1.390 (6)	1.38 (2)
N(1′)–C(2′)	1.319 (5)	1.389 (7)	1.346 (5)	1.333 (6)	1.37 (2)
C(2′)–C(3′)	1.386 (5)	1.342 (6)	1.379 (5)	1.413 (7)	1.36 (2)
Bond Angles (deg)					
N(2)–C(3)–C(4)	120.4 (2)	120.3 (4)	120.4 (3)	121.1 (5)	120 (1)
C(4)–C(3)–C(14)	121.0 (3)	124.8 (4)	125.3 (3)	125.0 (50)	120 (1)
C(3)–C(4)–C(10)	122.6 (3)	118.9 (4)	119.8 (3)	119.1 (5)	119 (1)
C(3)–C(4)–O(17)	122.1 (3)	123.9 (4)	123.8 (3)	123.9 (5)	123 (1)
O(15)–C(14)–N(16)	123.7 (3)	120.3 (4)	121.8 (3)	124.0 (5)	123 (1)
C(3)–C(14)–O(15)	120.8 (3)	124.4 (4)	122.8 (3)	121.5 (5)	122 (1)
C(3)–C(14)–N(16)	115.5 (3)	115.2 (4)	115.3 (3)	114.5 (4)	115 (1)
C(2′)–N(16)–C(14)	129.6 (3)	127.5 (4)	128.7 (3)	132.0 (5)	131 (1)
N(1′)–C(2′)–N(16)	112.7 (3)	119.7 (40)	112.5 (3)	122.4 (4)	119 (1)

[a] Key: I, neutral;[10] II, zwitterion;[1] III, anion;[12] IV, Cd complex (this work); V, Cu complex (this work).

through their carbonyl oxygen atoms O(5). The geometry of the five-membered chelate ring resembles closely those found in the octahedral complexes of Ni and Zn with *N*-(2-pyridyl)acetamide[9] where the amide nitrogen atom is protonated. The axial Cu–O bonds are weaker than the corresponding bonds in the Cd complex, as indicated by the long Cu–O(5) distances of 2.43 (1) Å.

The neutral piroxicam molecule undergoes several structural changes upon its complexation to the metal ions. A comparison of the metric parameters of piroxicam in its five known forms, namely the free neutral molecule,[10] the free zwitterion,[11] the free anion,[12] and the Cd and Cu complexes, is reported in Table V. As evidenced by the X-ray analysis, the deprotonation occurs at the enol oxygen site, while the amide nitrogen atom remains protonated. An increased contribution of the keto form leads to the observed shortening of the C(4)–O(17) bond length in the metal complexes when compared to that of 1.341 (5) Å found in the free neutral piroxicam molecule.[10] On the other hand, the C(4)–O(17) distances are close to that of 1.279 (4) Å observed in the zwitterionic form of the drug molecule.[11] The C(3)–C(4) bond shows a lengthening from 1.369 (4) Å in the neutral ligand[10] to 1.387 (5) Å in the anion[12] and to 1.396 (6) Å in the zwitterion[11] and the Cd complex. On the other hand, the C(3)–C(14) bond is longer in the free neutral molecule than in the other forms.

Minor changes occur for the C(14)–O(15) bond distance on going from one form to another. The C(14)–N(16) bond length increases in the order free neutral molecule (1.353 (4) Å), free anion (1.365 (4) Å), Cd complex (1.380 (6) Å) ≃ zwitterion (1.385 (6) Å). The values of the C(2′)–N(16) bond distances for the neutral molecule, the anion, and the Cd complex are slightly higher than that for the zwitterion form. Some significant changes are observed also for the pyridine ring. Here, the most noticeable feature is the lengthening of the C(2′)–C(3′) bond length from 1.342 (6) to 1.413 (7) Å in the zwitterion and the Cd complex, respectively. The N(1′)–C(2′) bond length of 1.389 (7) Å in the zwitterion is in turn contracted to 1.333 (6) Å in the Cd complex.

Furthermore, the analysis reveals an opening of the O(15)–C(14)–N(16) angle in the Cd complex (124.0 (5)°) relative to that in the zwitterion form (120.3 (4)°). A similar trend is also observed for the C(14)–N(16)–C(2′) angle.

The oxygen atom O(17) is involved in a strong intramolecular hydrogen bond N–H···O with the N(16)···O(17) distance of 2.581 (6) and 2.61 (2) Å in the Cd and Cu complexes, respectively.

(9) Scheller-Krattiger, V.; Scheller, K. H.; Sinn, E.; Martin, R. B. *Inorg. Chim. Acta* **1982**, *60*, 45.
(10) Kojic-Prodic, B.; Ruzic-Toros, Z. *Acta Crystallogr.* **1982**, *B38*, 2948.
(11) Bordner, J.; Richards, J. A.; Weeks, P.; Whipple, E. B. *Acta Crystallogr.* **1984**, *C40*, 989.
(12) Bordner, J.; Hammen, P. D.; Whipple, E. B. *J. Am. Chem. Soc.* **1989**, *111*, 6572.

Table VI. ^{13}C Relaxation Parameters Observed for the Piroxicam (0.15 M)–Cu(II) (6.0×10^{-4} M) System at 70 °C

nucleus	δ,[a] ppm	R_{1blank}, s^{-1}	R_{1p}, s^{-1}
C(14)	166.675	0.060	9.30
C(4)	159.157	0.105	2.40
C(2′)	149.880	0.090	6.31
C(6′)	145.900	0.690	6.11
C(4′)	139.201	0.780	1.00
C(9)	134.590	0.043	0.32
C(6)	132.843	1.070	0.27
C(7)	132.400	1.510	0.15
C(10)	128.717	0.053	0.31
C(5)	126.187	0.970	0.20
C(8)	123.577	0.860	0.20
C(5′)	119.850	1.420	2.56
C(3′)	115.773	0.770	2.94
C(3)	111.000	0.035	4.10

[a] ppm from TMS.

Similar hydrogen-bonding systems have also been observed in the zwitterionic forms of the drug.[11,12]

It should also be noted that the chelation of the drug molecule has little effect on the conformation of the benzothiazine system, as all the torsion angles describing the rings are similar to those found in the metal-free drug molecules.

IR Spectra. The infrared spectra for all the metal derivatives exhibit remarkable similarity. The amide I band (C=O stretching vibration) is moved from 1630 to about 1610 cm^{-1} on complexation with Cu(II), in agreement with the results of the X-ray structure analysis, which shows strong metal coordination to the amide oxygen atom. The sharp and strong band at 3340 cm^{-1} due to the O—H group of the free ligand is not detectable in the spectra of the metal complexes. This is consistent with the deprotonation of the enolate O—H group as shown by the X-ray analysis of the Cd and Cu derivatives. However the band at 1350 cm^{-1} attributable to the $>SO_2$ asymmetric stretching vibration undergoes a shift at higher energies (~30 cm^{-1}) upon complexation even if the $>SO_2$ group does not interact with the metal ion.

Visible and UV Spectra and Magnetic Data. The visible spectra obtained for the Co(II), Ni(II), and Cu(II) solid compounds crystallized from both DMSO and DMF are similar to those recorded in the respective solutions, indicating that similar structures occur in the two phases.

The visible spectrum of the pale green Ni(II) derivative has a band at 625 nm and a molar absorbivity of 8 cm^{-1} mol^{-1} dm^3 in DMSO at 25 °C.

The $Ni(Pir)_2 \cdot 2DMSO \cdot 2H_2O$ complex shows a weak band at 620 nm. The $Cu(Pir)_2 \cdot DMSO \cdot H_2O$ and $Cu(Pir)_2(DMF)_2$ crystals both show an absorption at 620 nm and a shoulder at 480 nm. The DMSO solution of the $Cu(Pir)_2 \cdot DMSO \cdot H_2O$ complex shows an absorption band at 666 nm with a molar absorbivity of 70.0 cm^{-1} mol^{-1} dm^3 at 25 °C.

The UV spectra of the metal derivatives in DMSO are alike (strong absorption occurs at 262 and 377 nm), but they differ from that of the parent compound. The long-wavelength absorption is red-shifted by ca. 45 nm, and its intensity is slightly enhanced relative to the spectrum of free HPir, indicating practically the same metal–ligand binding mode in the solution phase.

The magnetic moment values (μ_{eff}) at 24 °C for the Co(II) and Ni(II) solid compounds from DMSO, namely $Co(Pir)_2 \cdot 2DMSO \cdot H_2O$ and $Ni(Pir)_2 \cdot 2DMSO \cdot 2H_2O$ and the $Cu(Pir)_2 \cdot 2H_2O$ complex from methanol are 4.81, 3.26, and 1.90 μ_B, respectively. They are in agreement with 3, 2, and 1 unpaired electrons for the Co(II), Ni(II), and Cu(II) centers, respectively, and suggest a pseudooctahedral coordination geometry.

NMR Data. Further evidence for the Cu(II) coordination to O(15) and N(1′) atoms in DMSO solution comes from ^{13}C NMR experiments. The spin–lattice relaxation rate values (R_1) relevant to the HPir carbon atoms were analyzed in the absence and presence of the Cu(II) ions at 70 °C. The presence of the Cu(II) ions induces selective enhancements of R_1 values. As shown in Table VI, high paramagnetic contributions (R_{1p}) were observed for the C(2′), C(3), C(6′), and C(14) nuclei. In systems containing paramagnetic ions such as Cu(II) or Mn(II), the R_{1p} parameter is usually assumed to be dominated by the dipolar term because the scalar contribution is almost always negligible.[13] The dependence of R_{1p} on the metal–nucleus distance allows assignment of the paramagnetic binding sites. These R_{1p} data strongly confirm that the structure of the species under investigation in solution is similar to that in the solid state where the metal center is close to C(2′), C(3), C(6′), and C(14) atoms (see Figure 1). The analysis of the R_{1p} values for the C(3′), C(4′), and C(5′) nuclei reveals lower paramagnetic effects in comparison with those relevant to the C(2′), C(3), C(6′), and C(14) nuclei. Moreover the C(4′) nucleus shows a lower R_{1p} value with respect to the C(3′) and C(5′) carbon atoms. These results can also be explained by assuming a structure similar to that found in the solid state, where the C(4′) nucleus occurs in the para position with respect to the metal-bound N(1′) atom.

As the Cu–piroxicam complexes are very labile, the solution phase examined by using NMR techniques at 70 °C may contain several species. Since the piroxicam:Cu(II) molar ratio is 250 (see Table VI), we can assume that the $Cu(Pir)_2$ stoichiometry is the prevailing one. In addition to the pyridyl nitrogen and amide oxygen atoms, the enolate and the $>SO_2$ group oxygen atoms as well as the N(2) atom could act as donors. However, it should be pointed out that the R_{1p} values relevant to the C(5), C(6), C(7), C(8), C(9), and C(10) nuclei range between 0.15 and 0.32 s^{-1}, which indicates that the C(5)–C(10) ring experiences only very weak relaxation effects by the metal center. This observation rules out any appreciable coordination to the O(1), O(2), O(17), and N(2) atoms.

Concluding Remarks. The present study demonstrates that several first-row transition-metal ions are capable of forming stable chelates with piroxicam by employing the amide oxygen and pyridyl nitrogen atoms of the drug molecule. Recent spectroscopic studies on metal complexes with some other enolizable amides like 4-hydroxy-2-methyl-*N*-(5-methyl-3-isoxazolyl)-2*H*-1,2-benzothiazine-3-carboxamide 1,1-dioxide (isoxicam)[5] and 4-hydroxy-2-methyl-*N*-2-pyridyl-2*H*-thieno[2,3-*e*]-1,2-thiazine-3-carboxamide 1,1-dioxide (tenoxicam)[6] suggested that these antiinflammatory agents can act as monoanionic ligands through the enolate oxygen and amide oxygen atoms. Piroxicam, however, clearly does not follow the postulated pattern, adopting the N,O-coordination mode. Although an ambivalent ligating behavior cannot be excluded, it should be noted that the observed N,O-chelation could be a reflection of the preference of transition-metal ions to form intramolecular mixed-ligand complexes by binding to ligands with heteroaromatic N residues and O donors.[14,15]

Formation of the uncharged Cu–piroxicam species is of particular interest, since it has been shown[16] that such neutral Cu–drug complexes are essential for effective distribution of the pharmacoactive agents and maintaining the copper balance in blood plasma.

Acknowledgment. R.C. thanks Mr. F. Cecconi of ISSECC, CNR, Florence, Italy, for the magnetic susceptibility measurements. R.C. and C.R. thank Pfizer Italiana S.p.A. for the supply of piroxicam and the Italian Ministry of Public Education (MPI) for financial support. Part of the work has been done by M.S. at the Department of Chemistry, Northwestern University, Evanston, IL. We thank Professor T. V. O'Halloran, Northwestern University, for very useful discussions.

Supplementary Material Available: Tables of H atom coordinates and thermal parameters for all non-hydrogen atoms (2 pages); tables of observed and calculated structure factors (22 pages). Ordering information is given on any current masthead page.

(13) Espersen, W. G.; Martin, R. B. *J. Phys. Chem.* **1976**, *80*, 161.
(14) Sigel, H.; Martin, R. B. *Chem. Rev.* **1982**, *82*, 385.
(15) Sigel, H.; Fischer, B. E.; Prijs, B. *J. Am. Chem. Soc.* **1977**, *99*, 4489.
(16) Jackson, G. E.; May, P. M.; Williams, D. R. *J. Inorg. Nucl. Chem.* **1978**, *40*, 1227 and references therein.